Desalination and Water Treatment
www.deswater.com

doi: 10.5004/dwt.2023.29441

291 (2023) 1–11
April

Preparation of negatively charged glass surface modified filter media and its purification performance in drinking water

Quanbin Shi, Hongwei Zhang*, Peng Zhao, Yuan Zhang

School of Environmental Science and Engineering, Tianjin University, Tianjin 300072, China, Tel.: +86 13502171853; email: hwzhang@tju.edu.cn (H. Zhang), Tel.: +86 13312121918; email: Shiquanbin123456@163.com (Q. Shi), Tel.: +86 13920975826; email: zhp_tj@126.com (P. Zhao), Tel.: +86 17822001609; email: zhangyuan042055@163.com (Y. Zhang)

Received 24 October 2022; Accepted 8 March 2023

ABSTRACT

The filtering material is the key to determine filtering effect, the study found that the soda lime glass has high negative zeta potential, hydroxylation of soda lime glass medium, and then using γ-methylacryloxy propyl trimethoxysilane oxygen radicals silane (MPS) in three oxygen radicals silane coupling, and then the MPS of C=C key with C=C bond potassium salt of propyl methacrylate 3-sulfonate (SPM) polymer grafting modified filter material is prepared. The study shows that changing the amount of SPM can make the negative potential layer have different charges, and the potential can be as high as –148.19 mV. Under the condition of 50 mM and 1 mL/min, the graft-modified filter media showed a better filtration effect on specific pollutants, and the removal rates of Fe^{3+}, Mn^{2+} and NH_4^+ by 24-mesh graft-modified filter media were 62.18%, 71.53% and 61.85%, respectively. The removal rates of the above pollutants by 32-mesh grafted modified filter media can reach 85.72%, 87.49% and 79.69%, respectively. At the same time, the grafted modified filter media has good cycle stability, and the removal effect of 32-mesh modified filter media only decreased by 4.06% compared with the same period last year.

Keywords: Filtration; Glass filter material; Grafting modification; Removal efficiency

1. Introduction

Filter materials play a crucial role in the whole sewage treatment process. Traditional filter materials have very limited specific surface area, small interception and low void proportion, which can no longer meet the needs of production and life [1–3]. Modified filter media is a new treatment technology gradually emerging in the past 20 y [4]. Deng Deng and Mariia [5] used MnO_2, $MnO{\cdot}Fe_2O_3$, $CuO{\cdot}Fe_2O$ as a modifier, and ceramic particles, quartz sand and perlite as carriers to modify the filter media. They found that the modified filter media had a high removal efficiency for Fe^{2+}, and the maturity period of the material was significantly shortened. Lai et al. [6] took ferric nitrate as modifier material and used quartz sand as carrier to conduct modification research, and finally obtained filter material sand coated with iron layer. After placing it in the labeled filter column, it was found that the modified filter material showed a very high removal efficiency of copper ions, and the detection of effluent water quality found that the removal efficiency of copper ions was nearly 100%. From 20 y ago, foreign studies have begun to appear glass as the matrix of filter media, and it is found that recycled glass can effectively replace the most widely used quartz sand filter media in the current market [7–12]. Zhao et al. [13] used (3-aminopropyl)triethoxysilane (APTES) to surface modify the waste beer bottle glass filter material with a particle size of 0.8~1.2 mm after crushing and screening and prepared a new type of modified glass filter material. The removal rates of turbidity, humic acid and fine particulate matter by

* Corresponding author.

the modified glass filter material reached 62.5%, 67% and 66%, respectively, while the corresponding removal rates of quartz sand were only 37.5%, 55% and 10%. Liu et al. [14] grafted chitosan on glass microspheres to obtain a hybrid material capable of adsorbing transition metal ions. This hybrid material can successfully adsorb Cu^{2+}, Ag^{+}, Pb^{2+}, Fe^{3+} and other metal ions.

In this paper, sodium calcium glass as filter media matrix, SPM (potassium salt of propyl methacrylate 3-sulfonate) as monomer, MPS (γ-methylacryloxy propyl trimethoxysilane) as silane coupling agent, through grafting modification method on the surface of glass medium graft branched SPM polymer negative potential layer, The physical and chemical properties of the charged glass filter media with different charge were characterized and analyzed by changing the reaction reagent ratio. At the same time, the filtration performance, rejection rate and cycle experiment of the filter media before and after modification were carried out to explore the filtration removal performance of grafted modified filter media on Fe^{3+}, Mn^{2+} and NH_4^+.

2. Experimental materials and methods

2.1. Main instruments and reagents

2.1.1. Material

Hydrogen peroxide (AR, ≥30.0% Tianjin Fengchuan Chemical Reagent Technology Co., Ltd., Tianjin, China), γ-methylacryloxy propyl trimethoxysilane (97%, Aladdin Reagent (Shanghai) Co., Ltd., Shanghai, China), glacial acetic acid (AR, 99.5%, Tianjin Yuanli Chemical Co., Ltd., Tianjin, China), N,N′-dicyclohexyl carbodiimide (99.0%, Aladdin Reagent (Shanghai) Co., Ltd., Shanghai, China), 4-dimethylaminopyridine (99.0%, Aladdin Reagent (Shanghai) Co., Ltd., Shanghai, China), propyl methacrylate 3-sulfonate potassium salt (98.0%, Shanghai Maclin Biochemical Technology Co., Ltd., Shanghai, China), ammonium persulfate (99.99%, Aladdin Reagent (Shanghai) Co., Ltd., Shanghai, China), concentrated sulfuric acid (AR, 95%–98%, Tianjin Yuanli Chemical Co., Ltd., Tianjin, China), acetone (AR, 99.5%, Tianjin Yuanli Chemical Co., Ltd., Tianjin, China), ethanol (GR, 99.8%, Aladdin Reagent (Shanghai) Co., Ltd., Shanghai, China).

2.1.2. Equipment

Electronic analytical balance (ME204E/02, METTLER TOLEDO Instruments (Shanghai) Co., Ltd., China), electric heating blast drying box (DHG-9000, Shanghai Yiheng Scientific Instruments Co., Ltd., China), UV-Visible spectrophotometer (UV-2000, Unico(Shanghai) Instruments Co., Ltd., China), pH-meter (Lei CiPHS-25, Shanghai Yidi Scientific Instruments Co., Ltd., China), ultrasonic cleaner (SB25-12DTDN, Ningbo Xinzhi Biotechnology Co., Ltd., China), peristaltic pump (BT100S DT15, Baoding LEIFU Fluid Technology Co., Ltd., China), chromatography column (organic glass 1.6 cm × 20 cm, Shanghai Tongxing Glass Instrument Factory, China), surface potential analyzer (Zetasizer Nano ZS90 Malvern, Worcestershire, UK), Solid surface zeta potential analyzer (Zeta Phoremeter, CAD Instruments, France).

2.2. Preparation of modified filter media

Use ethanol to clean the raw material of glass beads with different sizes after screening, about 5–6 times; Put the cleaned glass bead raw material into the beaker containing deionized water, ethanol and acetone in turn and ultrasonic for 10 min; Put the raw material of glass beads after cleaning and ultrasonic into the "man-eating acid" solution, pickling in water bath (95°C) for 2 h; After pickling in the water bath, clean the sulfuric acid remaining in the glass beads with deionized water and put it into ethanol for storage.

The toluene solution of MPS (silane coupling agent) was prepared. The pickling glass bead raw material was immersed in the prepared silane coupling agent solution, the catalyst (DCC, DMAP) was added, and the solution was left for 24 h. The glass connected with silane coupling agent and ultrapure water was put in a large beaker, the water bath temperature was set to 80°C, and magnetic stirring was carried out. SPM and APS (ammonium persulfate) solution (functional monomer and initiator) were added, respectively after the temperature rose to 60°C, and the dripping time was controlled at about 30 min. The reaction was continued for 3~5 h after the completion of drip addition.

2.3. Study on the filtration performance of modified filter media

The background solution of specific ionic strength required for the test was prepared by NaCl. Two ionic strengths, 1 and 50 mmol/L were selected to simulate the ionic strength in the actual filtration environment. 1 and 5 mL/min were selected as the test filter speed, and the particle size of 24-mesh and 32-mesh were used as the test particle size. The initial concentration of iron ion solution, manganese ion solution and ammonia nitrogen solution was 0.3, 0.1 and 1 mg/L, respectively. In order to explore the filtration performance of the filter media before and after modification under the conditions of different ionic strength background solutions, particle size, filtration rate and pollutant types.

The test device is shown in Fig. 1. The filter material column is made of glass chromatography column (Shanghai Tongxing Glass Instrument Factory, China), which is 16 mm in inner diameter and 20 cm in length. The upper and lower ends of the column are equipped with nylon

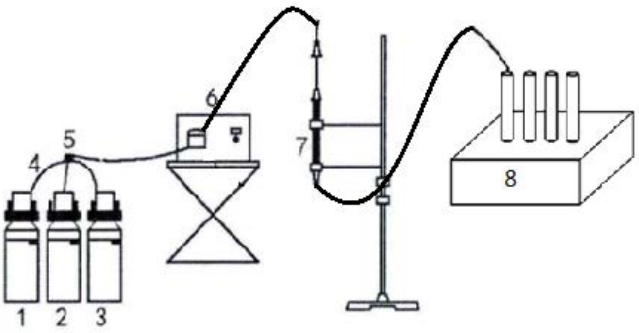

Fig. 1. Column test device (1. Background salt solution; 2. Colloidal particle suspension; 3. Deionized water; 4. Teflon air pipe; 5. Transfer valve; Peristaltic pump; 6. 7. Filling column; 8. Collection and detection system).

filter membrane with aperture of 100 μm to evenly disperse water flow and prevent the porous media material filled from leaking out. Porous media particles were added to the column several times. When the column was added at a height of about 2 cm each time, it was necessary to vibrate the column to discharge the bubbles between media particles, and at the same time, the porous media could be fully soaked to stabilize its porosity. Until the column was filled, the thickness of the filter layer was 10 cm, and the porosity of the packed column was measured. The bacterial solution and the background solution were passed from top to bottom through a peristaltic pump at a fixed filtration rate (1 and 5 mL/min). The peristaltic pump and the column were connected by Teflon tubes. The colloidal solution concentration that did not enter the filter column was denoted as C_0, and the solution concentration that flowed out of the filter column was denoted as C. The pollutant penetration curve was drawn with PV as the abscissa and C/C_0 as the ordinate. The migration ability of Fe^{3+}, Mn^{2+} and NH_4^+ can be reflected by the height of the platform of the penetration curve. The higher the platform, the stronger the migration ability. In addition, the shape of the penetration curve is also the key basis for discussing the migration mechanism of pollutants in porous media.

At the end of the filtration test, continue to analyze the concentration of pollutants retained in the filter media. The glass beads in the column were taken out in sections (the column length was 10 cm, and 2 cm was selected as a section, a total of 5 groups of test section data) and put into a bottle to add 10 mL of the ionic strength solution with the same as the filtration test, then put into a shaker and mix it for 30 min at the speed of 350 rpm. The eluted solution was taken for the spectrophotometric concentration test of iron ion, manganese ion and ammonia nitrogen. And compared with the initial concentration, the C/C_0 under different glass bead segments was finally obtained, and the interception effect of the modified filter material was further analyzed.

All the filter material after the filter column filtration test was collected and backwashed with ethanol and ultrasonic for 10 min. After repeated for 3 times, the cycle test was carried out under the condition of ionic strength of 50 mM and filtration flow rate of 1 mL/min. The cycle test was carried out for 5 consecutive times, and the C/C_0 when the filtration effect was approximately the peak value was compared under the condition of PV = 8. Then the cyclic filtration performance of modified filter media was explored.

3. Experimental results and discussion

3.1. Preparation of modified filter media

After hydroxylation of glass surface, toluene solution of MPS (silane coupling agent) was prepared (the ratio of toluene to MPS was, 10 mL toluene: Different amounts of MPS, and then the pH value was adjusted to 4 with acetic acid), the acid-washed glass bead raw material was immersed in the prepared silane coupling agent solution, and the catalyst (DCC, DMAP) was added. The dosage was 50 mg catalyst per 5 g glass slice, and the catalyst was allowed to stand for 24 h. In order to determine the optimal amount of MPS, seven groups of different proportions of MPS were added to the same weight glass slices, and a blank control group was set. The added proportion of MPS in samples 1–7 gradually increased, and the specific added amount is shown in Table 1.

The 0–7 samples obtained from the processing were characterized by infrared, respectively. In the infrared spectrum, No. 0 is the sodium–calcium glass samples treated with hydroxylation and not treated with MPS (OH-GS), and 1–7 are the sodium–calcium glass samples treated with different proportions of MPS (MPS-GS). It can be seen from the infrared spectrum that the two infrared peaks appearing at wavelengths around 560 and 806 cm^{-1} are caused by the symmetric stretching vibration and bending vibration of Si–O bond, respectively. After MPS treatment of OH-GS, the symmetric stretching vibration and bending vibration of Si–O bond were significantly weakened, and with the increase of MPS addition ratio, the vibration peak showed a trend of first weakening and then strengthening, and the characteristic peak of sample 2 weakened most obviously, as shown in Fig. 2.

In order to further compare the variation trend of characteristic peaks caused by different proportions of MPS addition, we amplified the 1,500~3,000 cm^{-1} band in Fig. 2, and the results are shown in Fig. 3. Through the amplified infrared spectrogram, it is found that the two peaks at 2,858 and 2,928 cm^{-1} are the characteristic peaks of methyl ($–CH_3$) and methylene ($–CH_2–$), respectively, 1,709 cm^{-1} is the characteristic peak of carbonyl group (C=O), and 1,640 cm^{-1} is the characteristic peak of carbon–carbon double bond (C=C).

Table 1
Glass sheets and MPS in different proportions

Serial number	GS (g)	MPS (mg)
0	2.82	0
1		2.5
2		3.5
3		5.5
4		6.5
5		7.5
6		10.5
7		45

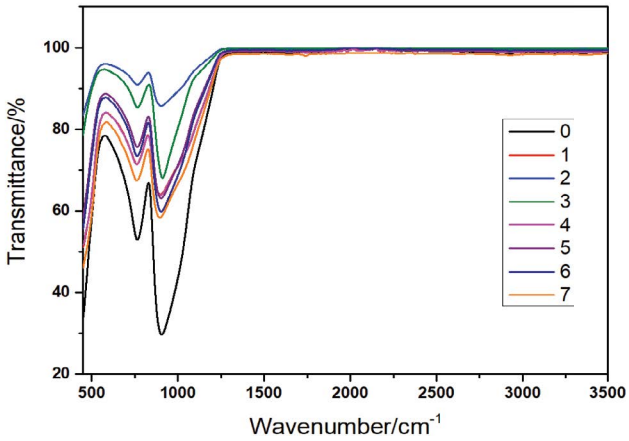

Fig. 2. Infrared spectra of MPS added in different proportions.

These organic functional groups can be found in the MPS structure, indicating that MPS has been successfully loaded onto the glass plate.

After the addition of MPS, the infrared characteristic peak still showed a trend of first weakening and then strengthening. According to the results shown in Fig. 3, the characteristic peak of 1,800~2,800 cm^{-1} in sample 2 shows obvious weakness, and the characteristic peak of MPS is the most obvious under the condition of MPS addition amount. When the proportion of MPS is gradually increased, the characteristic peak intensity shows an increasing trend. In the 1,800~2,800 cm^{-1} band, the clutter peak begins to appear, and the above results are consistent with the infrared characteristic peak results of Si–O in Fig. 2. In conclusion, the addition ratio of MPS in sample 2 was used as the best addition ratio for subsequent tests.

Because MPS has a double bond, it is theoretically possible to polymerize with SPM to negatively charge the slide surface. Connect the glass with silane coupling agent and ultrapure water into a large beaker, the water bath temperature was set to 80°C, and magnetic stirring was carried out. SPM (potassium salt of propyl methacrylate 3-sulfonate) and APS solution (functional monomer and initiator) were added, respectively after the temperature rose to 60°C, and the dripping time was controlled at about 30 min. The reaction was continued for 3~5 h after the completion of drip addition. In order to determine the optimal ratio of SPM and APS, the following experimental studies were conducted.

The samples with the best MPS addition amount were selected for subsequent tests. In this stage, SPM and APS with different addition ratios were used to carry out double bond polymerization reactions on the MPS treated samples, respectively. Seven groups of different SPM and APS addition ratios were set, and the SPM and APS addition ratio was taken as the only variable, as shown in Table 2. The 7 groups of samples after the reaction were tested by infrared, and the infrared test results were shown in Fig. 4. The experiment found that the infrared spectrum of the samples after SPM treatment was basically consistent with that after MPS treatment. In order to further understand the changes in samples after SPM and APS treatment, we amplified the 1,500~3,000 cm^{-1} band in Fig. 4, and the results are shown in Fig. 5. 2,856 and 2,925 cm^{-1} are the characteristic peaks of methyl ($–CH_3$) and methylene ($–CH_2–$), respectively, 1,709 cm^{-1} is the characteristic peak of carbonyl group (C=O), 1,640 cm^{-1} is the characteristic peak of carbon–carbon

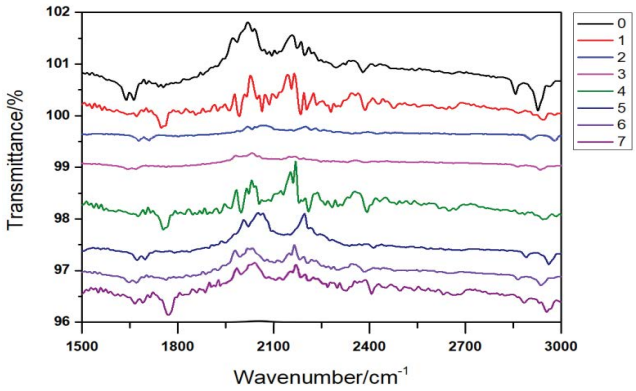

Fig. 3. Infrared local amplification spectra of MPS added in different proportions.

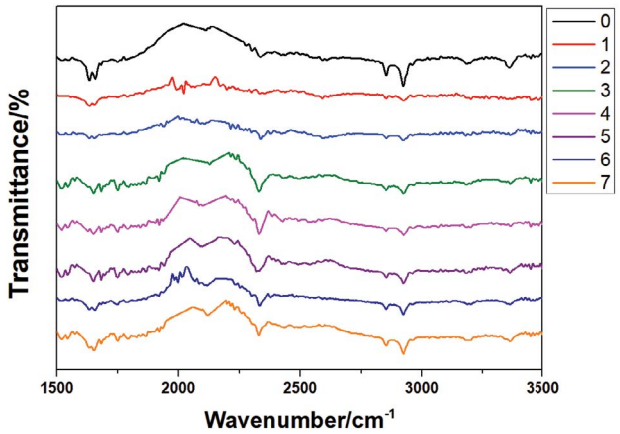

Fig. 5. Infrared local amplification spectra of SPM and APS in different proportions.

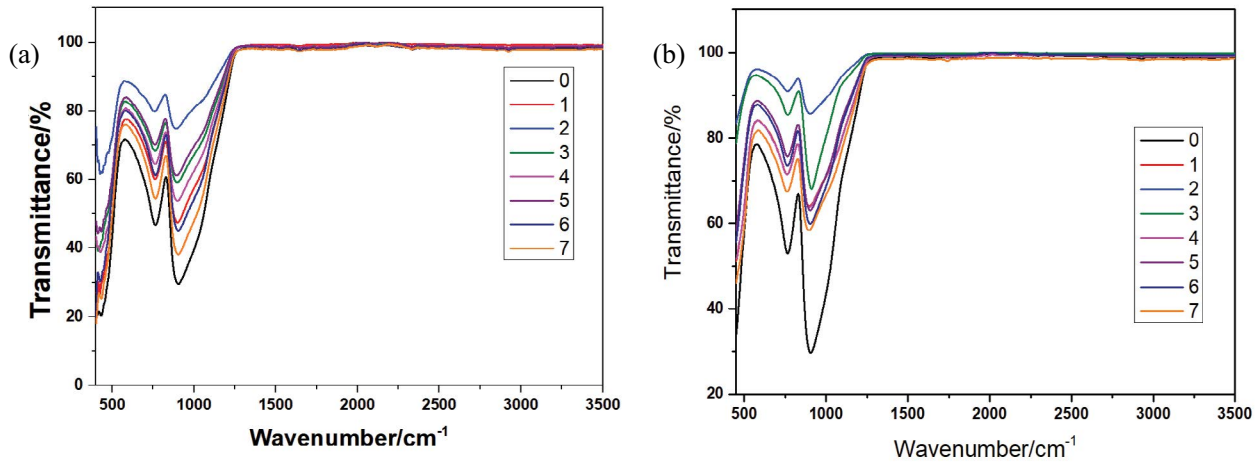

Fig. 4. Infrared spectra of SPM and APS in different proportions.

double bond (C=C), these organic functional groups are the characteristic peaks of MPS. It is still obvious in SPM and APS treated samples. In view of this result, it is considered that the glass surface with active chemical groups after MPS silanization can react with monomers or oligomers with special functions under certain conditions. The peaks at 2,334 and 3,365 cm^{-1} are divided into S=O and S–O characteristic peaks. Therefore, it is judged that SPM has been loaded on the sample. With the increase of the proportion of SPM added, the characteristic peaks show a trend of first enhancement and then stabilization, and the characteristic peaks in sample 3 have been more obvious. APS used in this study are free radical initiators, which promote the occurrence of chemical reactions. In order to reveal the influence of different amounts of APS on the experimental results, different proportions of APS were prepared for the experiment. The specific proportions are shown in Table 3.

Samples with different APS addition ratios were analyzed by infrared spectroscopy to obtain Fig. 6. The two infrared peaks around 560 and 806 cm^{-1} in Fig. 6a correspond to the symmetric stretching vibration and bending vibration of Si–O bond, respectively. It can be seen that APS has relatively little influence on the peak intensity, and there is little difference in peak intensity. At the same time, it can also be seen from Fig. 6b that different APS addition amounts have relatively little influence on the atlas of the sample in the bands of 1,500~3,500 cm^{-1}. Therefore, it is inferred that APS in this experiment, as an initiator, can promote the reaction of MPS and SPM. A small amount of APS can trigger the reaction. When APS is added in excess, the characteristic peak intensity does not change much. Therefore, we choose to add a small amount of APS in the subsequent experiment, and will not conduct in-depth analysis of APS in the subsequent experiment.

In order to further clarify the potential changes of samples with different addition amounts, zeta potential test was performed on glass samples, respectively. Sample No. 0 was a glass sample treated with MPS but not treated with SPM. The zeta potential test results are shown in Table 4. According to the zeta potential data, the average potential of the glass sample with serial number 3 can reach –148.19 mV, which is the highest value among samples with serial numbers 1–7. As the proportion of SPM increased gradually, the zeta potential showed a trend of gradual decrease. After excessive SPM addition, the zeta potential was lower than that of the original sample without SPM addition.

Table 2
Glass sheets and SPM and APS in different proportions

Serial number	SPM (mg)	APS (mg)	Glass sheet	Ultrapure water
1	4	4		
2	7	7		
3	11	11		
4	15	15	2.82 g	100 mL
5	25	25		
6	30	30		
7	50	50		

Table 3
APS ratio to be added

Serial number	Glass sheet (g)	MPS (mg)	SPM (mg)	APS (mg)
1–1	1.41	1.75	10	0
1–2				1
1–3	1.41	1.75	10	5
1–4				10

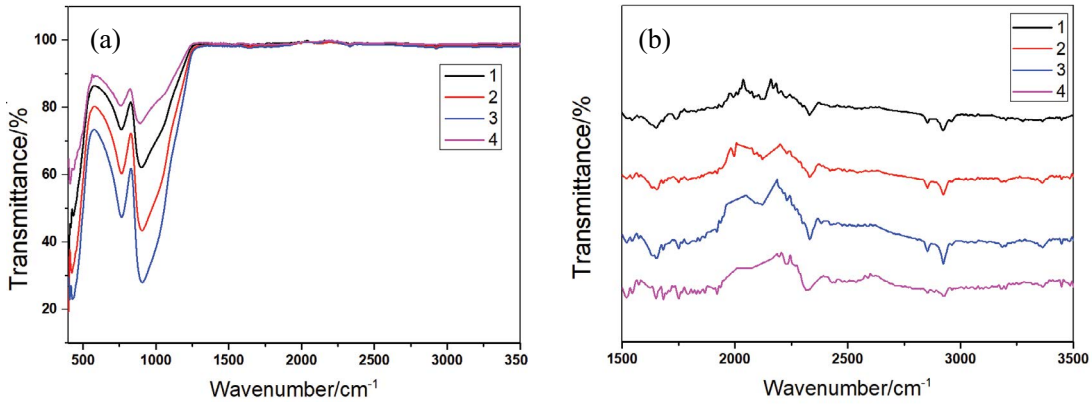

Fig. 6. Infrared spectra of APS added in different proportions: (a) full spectrum and (b) local amplified spectrum.

Table 4
Zeta potential test results

Sample	0	1	2	3	4	5	6	7
Zeta potential (mV)	–94.95	–118.47	–139.31	–148.19	–130.70	–113.58	–90.95	–72.78

The X-ray photoelectron spectroscopy (XPS) analysis results of the glass filter media before and after modification are shown in Fig. 7. Meanwhile, the percentage of each element in the two groups of glass medium samples before and after grafting modification is obtained, as shown in Table 5. It can be seen that the main elements of glass before and after modification are basically unchanged, mainly C, O, Si, Na, Ca, Mg. SiO_2 is the main component of glass structure and is the best glass forming body. In the glass microstructure, SiO_2 takes SiO_4 tetrahedron as the structural unit to form an irregular continuous network structure, which becomes the "skeleton" of glass. Na_2O can reduce the melting temperature of glass and is a very good flux. The presence of CaO can greatly improve the mechanical strength, hardness and chemical stability of glass. At the same time, appropriate addition of MgO can reduce the high temperature viscosity, crystallization tendency and crystallization speed of glass, which plays an important role in improving the mechanical strength, chemical stability and thermal stability of glass. However, the content of MgO should be controlled at a moderate level and should not be too high. As the raw material of the glass medium is sodium–calcium glass, according to the grafting modification principle, the main elements of the negative potential layer on the glass surface are C, O, S, etc. After comparison and analysis, it can be concluded that the carbon content is increased compared with that before modification, but the amplitude is not obvious, and it can be concluded that SPM monomer grafting is successful.

By XPS analysis, which can be quantitatively various glass medium samples after graft modification of atoms of each element percentage and weight percentage, compared with XPS needs to undertake the ground to a powder sample determination, determination of energy-dispersive X-ray spectroscopy can directly on the surface of the glass element content changes, more directly reflects the negative potential layer after graft modification of elements. As can be seen from Table 6, compared with raw sodium–calcium glass sheets, due to silane coupling and functionalization, many Si–O chemical bonds are attached to the surface of the medium. Therefore, the contents of Si and O elements are significantly increased compared with the raw glass sheet, and the contents of other S and K elements will also increase with the increase of the proportion of monomer SPM. The two trends are generally consistent, which indirectly proves the conclusion that SPM monomer grafting is successful.

The surface morphologies of the unmodified glass medium and the negatively charged glass medium after graft modification observed by scanning electron microscopy are shown in Fig. 8. Can be seen from the diagram, modification of the surface of the glass is very smooth, from multiples

Table 5
Changes in the element content of glass samples before and after grafting modification

Type of element	Before modification (at.%)	After modification (at.%)
C	28.08	30.08
O	43.26	44.22
Si	19.28	18.66
Ca	1.36	1.32
Na	6.3	6.12
Mg	0.72	0.60

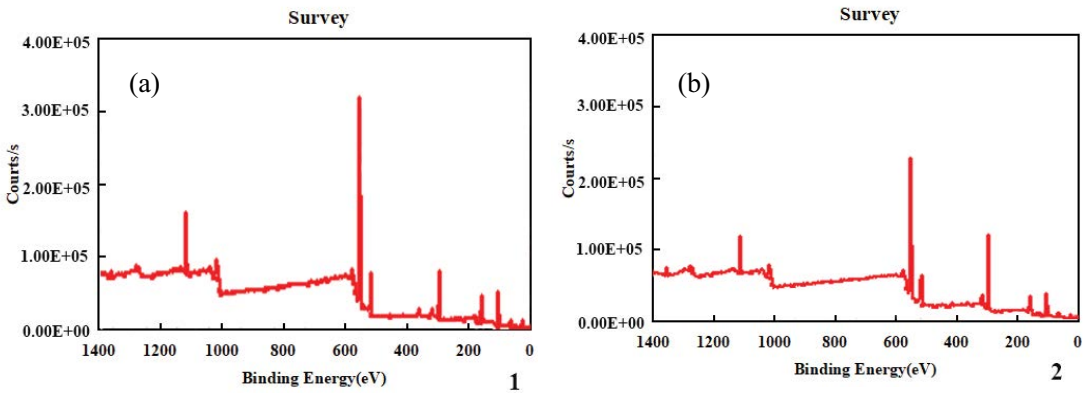

Fig. 7. X-ray photoelectron spectroscopy map of glass samples before and after grafting modification (a) unmodified glass medium and (b) negatively charged glass medium after grafting modification.

Table 6
Energy-dispersive X-ray spectroscopy test results of glass dielectric surface under different drug ratios

Elementary composition	C		O		Si		S		K	
	wt.%	at.%	wt.%	at.%	wt.%	at.%	wt.%	at.%	wt.%	at.%
Soda-lime glass	14.51	20.54	60.50	64.33	24.99	15.13	0.00	0.00	0.00	0.00
After grafting modification	6.16	10.42	41.04	52.14	48.30	34.95	1.35	0.86	3.15	1.64

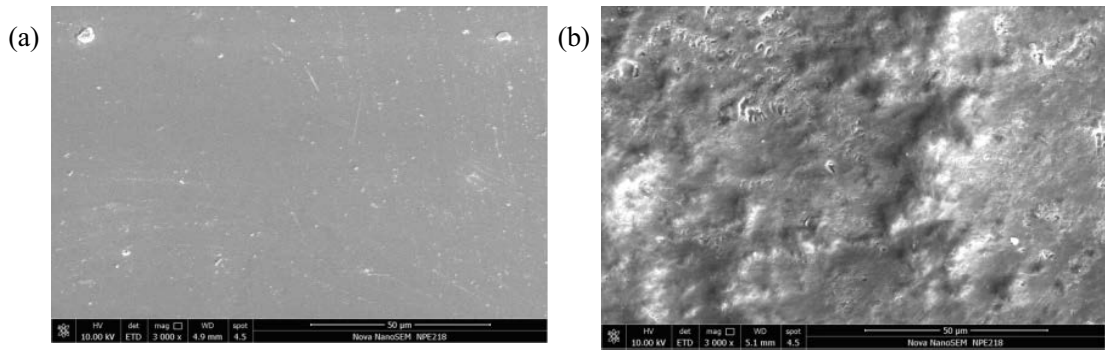

Fig. 8. Scanning electron microscopy images of glass samples before and after grafting modification (a) unmodified glass medium and (b) grafted modified negatively charged glass medium.

larger field of vision, can be found that the graft modification of glass dielectric surface roughness increases, and can be clearly observed synaptic morphology, this shows that in the substrate surface grafting of polymers are branched state, and state of the polymer, It lays a foundation for the fabrication of electrified glass filter material.

Table 7 shows the contact angle analysis results of glass medium surface before and after grafting modification. As can be seen from Table 7, compared with the raw sodium–calcium glass sheet, the grafted modified glass medium underwent silane coupling and functionalization, and many Si–O chemical bonds and negative potential layers were attached to the surface of the medium, which greatly improved the hydrophilicity. At the same time, compared with the raw material sodium–calcium glass sheet, the modified glass medium is coupled and functionalized with silane. Since SPM monomer contains negative electric groups, the negative value of zeta potential will increase with the increase of the proportion of SPM monomer. The above experimental results indirectly proved the conclusion that SPM monomer grafting was successful.

Table 7
Test results of glass medium surface under different drug ratio

Sample	Raw material sodium calcium glass sheet	Grafted modified glass sheet
Contact angle	69.32–73.92	17.58–18.74
Zeta potential (mV)	–94.9517 mV	–148.19 mV

3.2. Study on filtration performance of modified filter media

By analyzing the filtration test results, it can be found that the filtration effect of grafted modified filter media on Fe^{3+}, Mn^{2+} and NH_4^+ is significantly increased. When the ionic strength of the background solution is 50 mM and the filtration flow rate is 1 mL/min, the penetration plateau curve C/C_0 is the lowest, that is, the filtration effect of removing pollutants is the best. Through the test, it was found that the optimal test conditions for removing each pollutant were NaCl solution ionic strength 50 mM and flow rate 1 mL/min. This is because as the ionic strength of the background solution increases, the zeta potential of the surface layer of the negatively charged glass filter material after grafting modification will increase, which leads to the enhancement of the electrostatic attraction between the porous medium and the ions of the pollution material. In addition, when the filtration speed is slow, the pollutant solution can more fully interact with the filter media, which is conducive to improve the removal efficiency of filtration; At the same time, compared with the ionic strength, the filtration rate has a stronger influence on the filtration effect.

At the same time, through multiple groups of test analysis found that the filter material filtration effect under 32-mesh particle size is significantly higher than the filter material filtration effect under 24-mesh particle size, at the same time, the test found that the impact of particle size on the filtration effect is significantly higher than the background solution ionic strength and filter speed index. This is because the filter media with small particle size has a larger specific surface area and is more likely to react with Fe^{3+}, Mn^{2+} and NH_4^+ in aqueous solution. At the same time, the smaller the particle size, the narrower the gap of the filter material in the filter column, so that the filtering effect is further enhanced.

As shown in Fig. 9a–d, under the condition of 50 mM and 1 mL/min, the removal rate of Fe^{3+} by 24-mesh grafted modified filter media can reach 62.18%, and the removal rate of Fe^{3+} by 32-mesh grafted modified filter media can reach 85.72%. The filtration effect of grafted modified filter media is greatly improved, indicating that the modified filter media shows higher filtration performance. This is because the surface of the glass is coated with active chemical groups after silanization, which is easy to react with monomers or oligomers with special functions under certain conditions [15–18]. After modification, the surface of the filter material has a lot of negative potential, which is helpful to react with metal cations and further improve the filtration effect of the material. Fig. 9e–h shows the removal results of Mn^{2+} by the filter media before and after grafting modification. Under the condition of 50 mM and 1 mL/min, the removal rate of Mn^{2+} by the 24-mesh grafted modified filter media can reach 71.53%, and the removal rate of Mn^{2+} by the 32-mesh grafted modified filter media can reach 87.49%. The removal rate of Mn^{2+} by modified filter media is better than that of Fe^{3+} by modified filter media. Fig. 9i–l shows

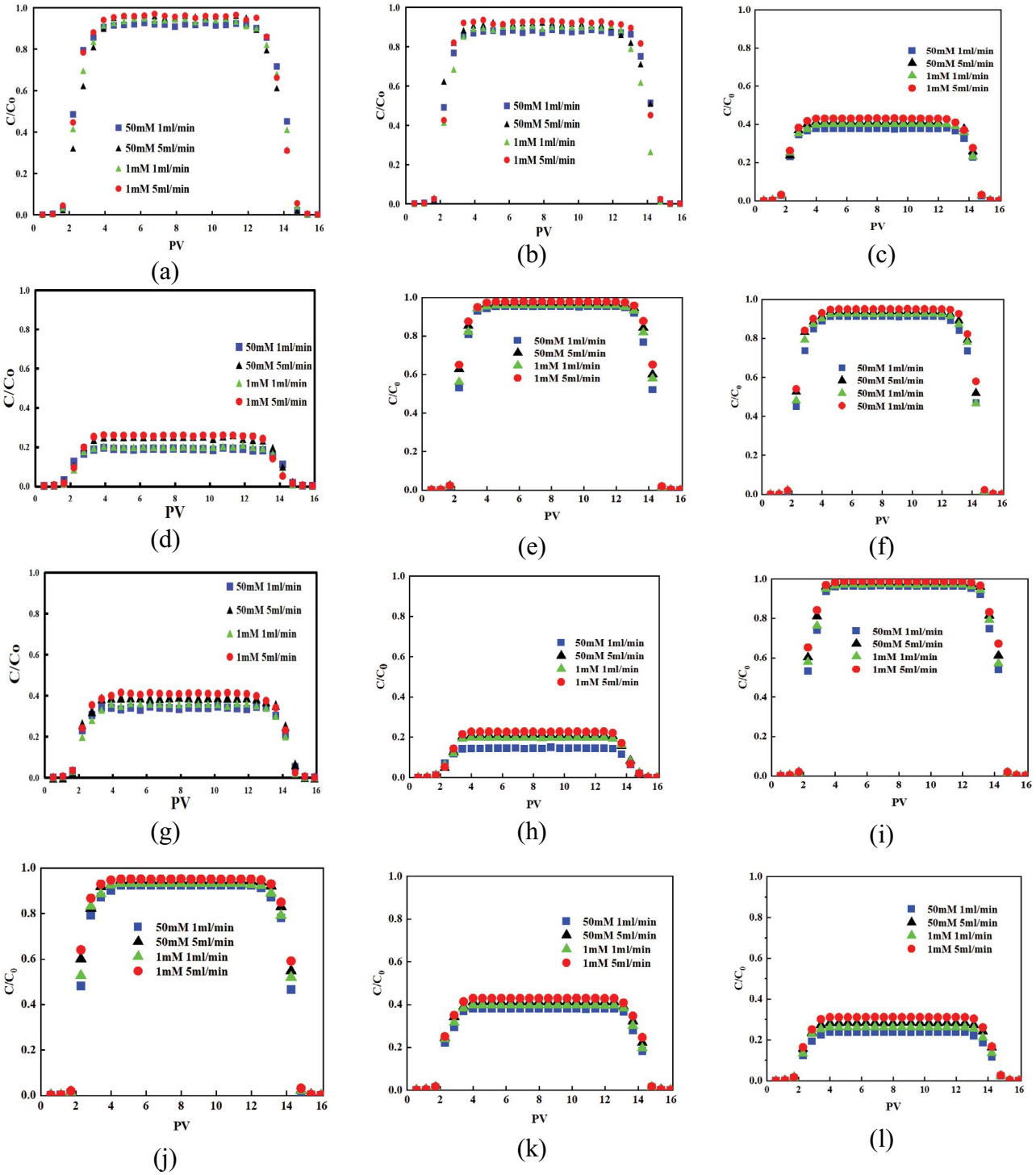

Fig. 9. Penetration plateau curves of metal iron with different filter media at different flow rates and ionic strengths: (a) unmodified 24-mesh Fe^{3+}, (b) unmodified 32-mesh Fe^{3+}, (c) modified 24-mesh Fe^{3+}, (d) modified 32-mesh Fe^{3+}, (e) unmodified 24-mesh Mn^{2+}, (f) unmodified 32-mesh Mn^{2+}, (g) modified 24-mesh Mn^{2+}, (h) modified 32-mesh Mn^{2+}, (i) unmodified 24-mesh NH_4^+, (j) unmodified 32-mesh NH_4^+, (k) modified 24-mesh NH_4^+ and (l) modified 32-mesh NH_4^+.

the removal results of NH_4^+ by the filter media before and after grafting modification. Under the condition of 50 mM and 1 mL/min, the removal rate of NH_4^+ by the filter media with 24-mesh grafting modification can reach 61.85%, and the removal rate of NH_4^+ by the filter media with 32-mesh grafting modification can reach 79.69%.

At the same time, the data analysis of the penetration ratio of different filter media to different pollutants under

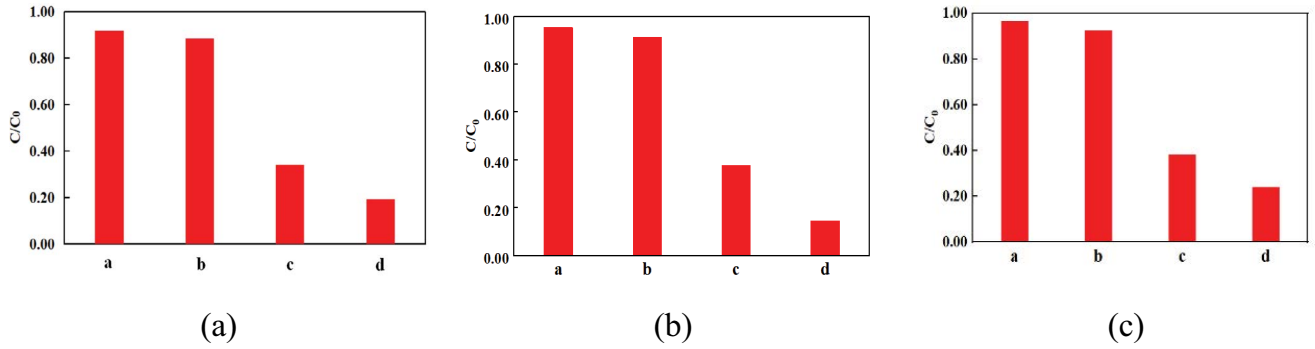

Fig. 10. Penetration ratio of different filter media to different pollutants under the best conditions (50 mM and 1 mL/min) (a) unmodified 24-mesh, (b) unmodified 32-mesh, (c) modified 24-mesh, (d) modified 32-mesh: (a) Fe^{3+}, (b) Mn^{2+} and (c) NH_4^+.

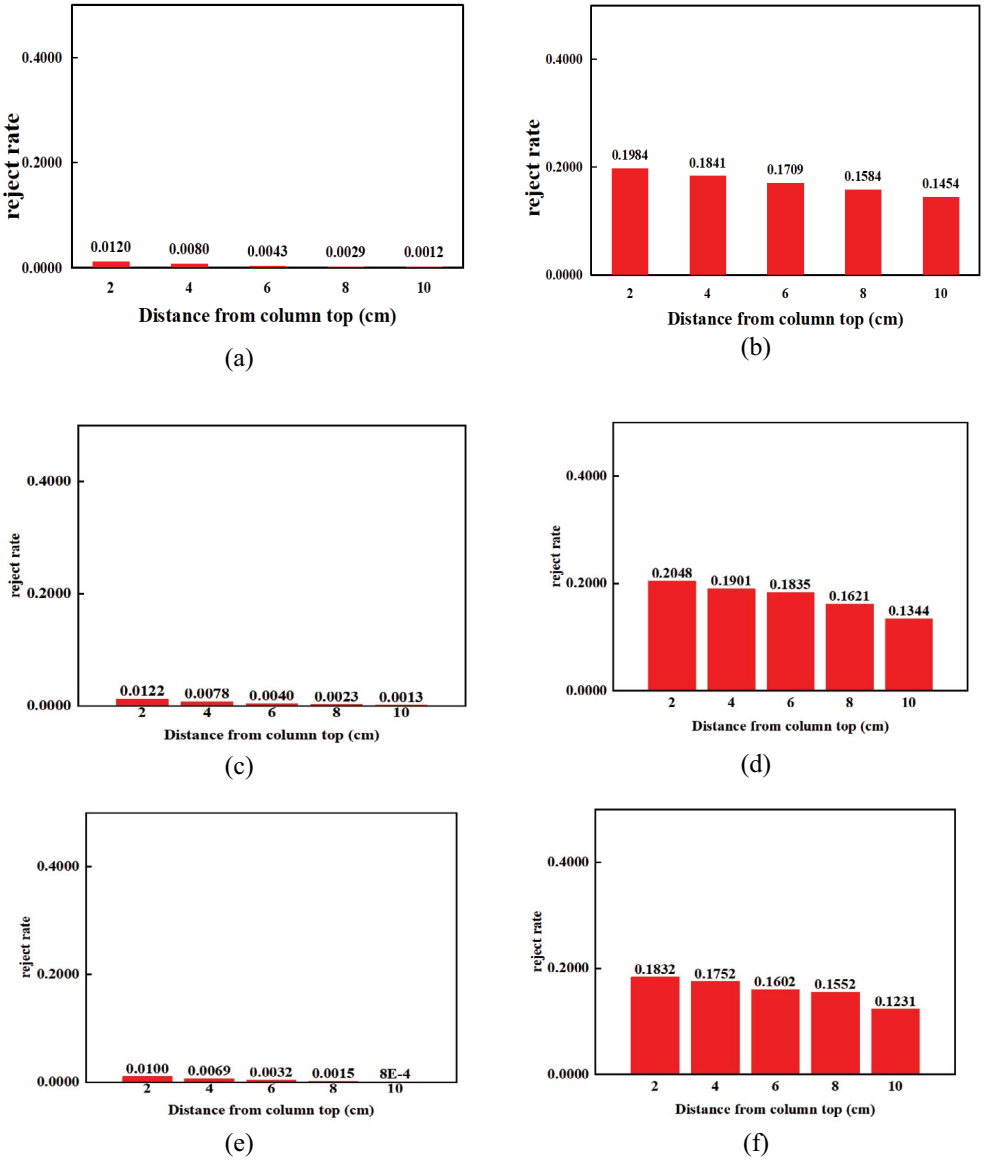

Fig. 11. Interception ratio of glass beads (32-mesh) to pollution substances before and after modification: (a) 32-mesh unmodified filter material Fe^{3+}, (b) 32-mesh modified filter material Fe^{3+}, (c) 32-mesh unmodified filter material Mn^{2+}, (d) 32-mesh modified filter material Mn^{2+}, (e) 32-mesh unmodified filter material NH_4^+ and (f) 32-mesh modified filter material NH_4^+.

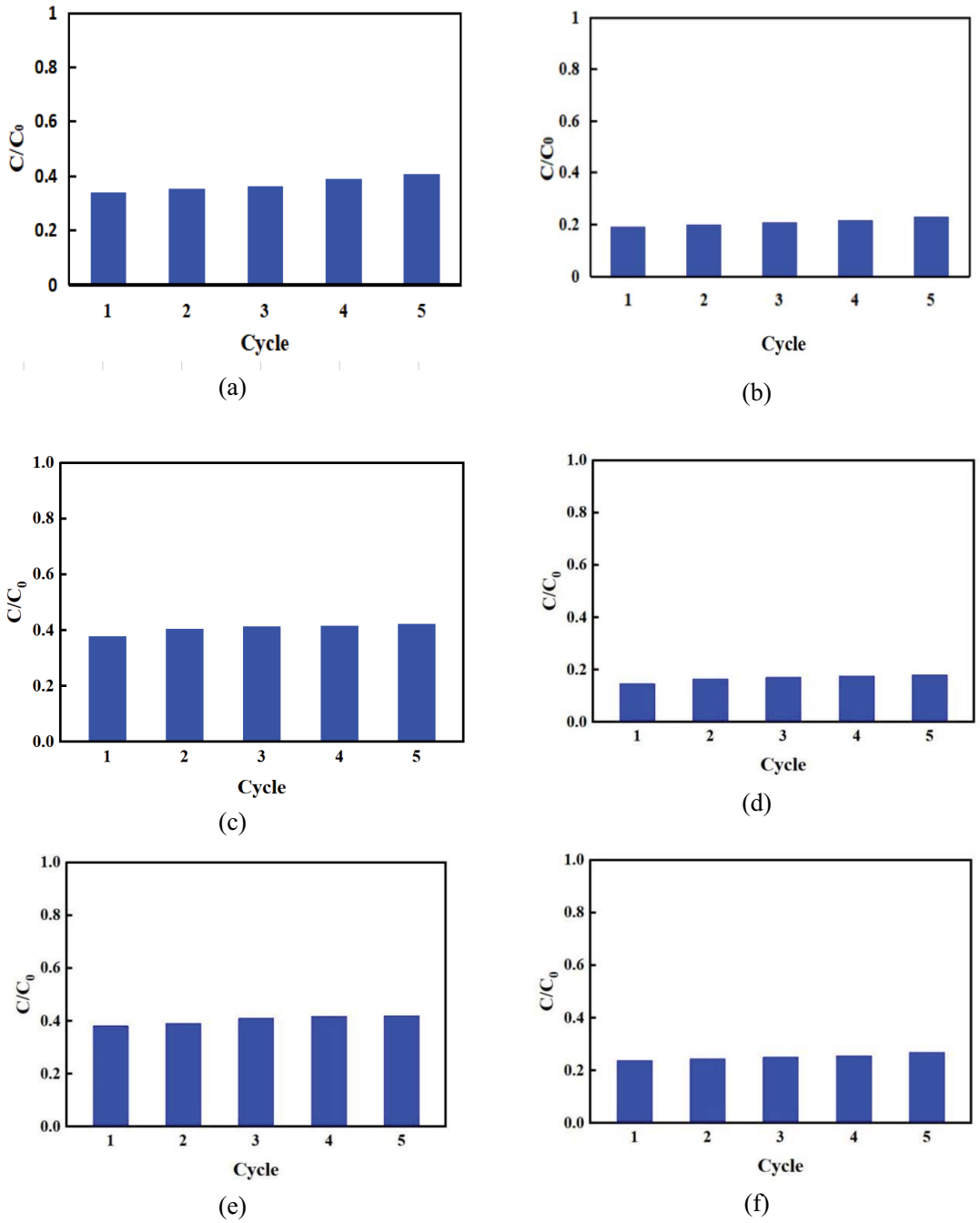

Fig. 12. Cycle analysis of modified filter media: (a) 24-mesh modified filter media Fe^{3+}, (b) 32-mesh modified filter material Fe^{3+}, (c) 24-mesh modified filter material Mn^{2+}, (d) 32-mesh modified filter material Mn^{2+}, (e) 24-mesh modified filter material NH_4^+ and (f) 32-mesh modified filter material NH_4^+.

the best conditions (50 mM and 1 mL/min) can confirm the above conclusion again, as shown in Fig. 10. The eluted solution of 32-mesh grafted modified filter media was used for spectrophotometric Fe ion concentration test, and compared with the initial concentration, the C/C_0 under different glass bead segments was finally obtained, and the interception effect of the modified filter material was further analyzed. As can be seen from Fig. 11, among the five glass bead segments of 1–10 cm, the 0–2 cm segment has the highest rejection rate, and then the rejection rates of the 2–4 cm, 4–6 cm, 6–8 cm and 8–10 cm segments gradually decline. This is because the solution containing heavy metal ions first passes through the 0–2 cm glass bead segment, and the concentration of heavy metal ions in the solution is the highest at this time, so it is easier for more metal iron ions to be trapped when passing through the glass bead segment of the filter material. With the deepening of the depth, the concentration of iron ions gradually decreases. In addition, it is found that

the modified filter media has a more obvious interception effect on iron ions. The interception rate of 0–2 cm glass beads is 19.84%, while the interception rate of unmodified filter media is only 1.20%, which is increased by 15.53 times. The rejection rate of 8–10 cm glass bead segment after modification is 14.54%, while that without modification is only 0.12%. Rejection data are also consistent with filtering results, which also indicates that the modified filter media presents better filtering effect compared with the unmodified filter media.

Under the premise of ionic strength of 50 mM and filtration flow rate of 1 mL/min, the cycle test was carried out for five consecutive cycles. At the same time, the filtration effect under the condition of PV = 8 was similar to the peak C/C_0, so as to explore the cycle filtration performance of the modified filter media. Fig. 12 shows the cyclic performance analysis of grafted modified filter media with different particle sizes. It can be seen from Figs. 1–12 that the cyclic stability of the modified filter media is better. The removal effect of 24-mesh modified filter media decreased by 6.35%, while the removal effect of 32-mesh modified filter media only decreased by 4.06%. After 5 cycles of material use, the removal effect of 24-mesh modified filter media can still reach more than 65%, and the removal effect of 32-mesh modified filter media is greater than 75%. Because the filter media still shows high removal efficiency after 5 cycles, it can be concluded that the modified filter media has better cycle stability performance, and has a good industrialization prospect.

4. Conclusion

Based on the existing filter material having poor filtration effect, unstable performance and other defects, this paper successfully prepared grafted modified filter material using sodium calcium glass as raw material. The graft modification of glass filter medium with negative potential layer was studied, and a series of characterization analysis of glass samples were carried out. The results show that the structure of sodium–calcium glass is stable and controllable, and it can be used as the matrix of filter material. By grafting modification technology, the amount of branched polymer was successfully controlled, so that it has the function of negative potential layer, and the maximum charge can reach –148.19 mV. The filtration and adsorption properties were studied, and the modified filter media were further tested and analyzed. A series of filtration and adsorption properties of untreated glass beads, acid-treated glass beads and grafted glass beads were studied. The target pollutants were Fe^{3+}, Mn^{2+} and NH_4^+. The experimental results show that the grafted modified filter media has a better filtration effect on specific pollution substances under the conditions of 50mM and 1 mL/min. The removal rate of Fe^{3+}, Mn^{2+} and NH_4^+ can reach 62.18%, 71.53% and 61.85%, respectively. The removal rate of Fe^{3+} by 32-mesh graft-modified filter media can reach 85.72%, and the removal rate of Mn^{2+} by Mn^{2+} can reach 87.49%. The removal rate of Mn^{2+} by modified filter media is better than that by modified filter media, and the removal rate of NH_4^+ by 32-mesh graft-modified filter media can reach 79.69%. At the same time, the grafted modified filter media has good cycle stability, and the removal effect of 32-mesh modified filter media only decreased by 4.06%.

Acknowledgements

This work was financially supported by the Longshan Academic Talent Research Supporting Program of SWUST (18LZX447) and the biofilm research & innovation consortium from the College of Science and Engineering, Flinders University for supporting this research, respectively.

References

[1] D.E. Fontes, A.L. Mills, G.M. Hornberger, Application of modified filter media in water treatment, Appl. Environ. Microbiol., 57 (1991) 2473–2481.
[2] M. Ye, J. Pan, P. Chen, Modified manganese sand filter materials processing water containing ammonia nitrogen of high manganese iron optimal operation parameters study, J. Jiangsu Water Conserv., 9 (2018) 11–15.
[3] D.F.R.R. Paula, D.S.C. Paiva, A.H. Cezar, B. Aanré, A.M. Lopes, *In-situ* evaluation of filter media modified by biocidal nanomaterials to control bioaerosols in internal environments, Water Air Soil Pollut., 232 (2021) 119–130.
[4] Y. Skolubovich, E. Voytov, A. Skolubovich, Liliallyina, Clear of underground water from ferric and manganese modified filtering material active pink sand, IOP Conf. Ser.: Earth Environ. Sci., 90 (2017) 25–42.
[5] H. Deng, T. Mariia, Research of efficiency of water purification-exchange resin from iron compounds using modified filter media, Eastern-European J. Enterp. Technol., 2 (2016) 32–42.
[6] J. Lai, J. Lu, S. Wang, Copper coated iron sand filter to remove the water research, Water Supply Drain., 46–48 (2015) 83–86.
[7] M. Ye, J. Pan, P. Chen, Study on optimal operation parameters of modified manganese sand filter media for treatment of high ferric manganese water containing ammonia nitrogen, Mod. Commer. Trade Ind., 22 (2010) 278–279.
[8] W. Liu, C. Wu, J. Ye, Modified filter material in addition to Cr(VI) efficiency and influencing factors of study, J. Chem. Sci. Technol., 4 (2009) 26–28.
[9] D. Li, J. Huang, C. Wu, J. Liang, M. Huang, Z. Wang, Biological-nanometer modified filter material handling ammonia nitrogen and COD (Mn) study, Water Treat. Technol., 44 (2018) 124–128.
[10] J. Hu, C. Wang, X. He, L. Shao, D. Li, K. Yin, M. Wu, Study on the influence factors of the removal of iron and manganese ions from mine water by modified volcanic rock filter media, Chin. J. Environ. Eng., 3 (2009) 1199–1202.
[11] J. Lu, L. Sun, X. Zhao, Y. Li, Y. Li, L. Zhang, Adsorption and filtration removal of phosphorus from water by a new type of iron-modified sand filter, J. Tianjin Univ., 43 (2010) 1115–1122.
[12] L. Liu, X. Tao, Y. Gu, Experimental study on the treatment of oilfield wastewater by AFM filter media, Guangzhou Chem. Ind., 47 (2019) 85–86.
[13] S. Zhang, Z. Zhao, W. Peng, Z. Mai, J. Zhou, J. Shi, T. Wan, Progress in the study of sand filter technology in water treatment, J. Mod. Chem. Ind., 46–48 (2017) 153–156.
[14] X. Shen, X. Yan, Y. Lin, Y. Xu, R. Liu, A new type of steel slag base unburned ceramsite filter material preparation and its performance study, J. Environ. Eng. Technol., 10–18 (2020) 37–43.
[15] P. Lei, L. Li, S. Cai, S. Chen, Water treatment filter material gradation said method at home and abroad comparative study, Water Supply Drain., 58 (2022) 1–7.
[16] M.M. Michel, L. Reczek, D. Papciak, M. Wodarczyk-Makua, T. Siwiec, Y. Trach, Mineral materials coated with and consisting of MnO*x*-characteristics and application of filter media for groundwater treatment: a review, Materials, 13 (2020) 13–24.
[17] D. Hu, B. Wei, X. Guo, Study on the relationship between surface wettability, surface free energy and hydrophilicity of water treatment filter media, Guangdong Chem. Ind., 44 (2017) 68–70.
[18] W. Zhang, R. Dai, L. Wu, F. Liu, R. Chen, Petrochemical wastewater biological treatment of residual sludge water treatment filter material preparation research, J. Mod. Chem. Ind., 5 (2014) 130–133.